International Journal of Concrete Structures and Materials

RESEARCH

Open Access

Corrosion Characteristics of Prestressing Strands and Reinforcing Bars Under Accelerated Corrosion Conditions

Tae-Hoon Kim[1*], Ki-Young Eum[1], Chang-Ho Sun[2] and Ick-Hyun Kim[2]

Abstract

This study investigates the corrosion characteristics of prestressing strands and reinforcing bars using mold specimens. These components such as prestressing strands and reinforcing bars are critical for the durability and structural safety of prestressed and reinforced concrete structures, as they bear loads in tensile regions. Prestressing strands, which are constantly under high tensile stress, are particularly susceptible to corrosion. The presence of poorly compacted grout or the infiltration of de-icing agents from an upper girder can accelerate corrosion in these strands, potentially leading to their failure and significantly compromising structural safety. The extent of corrosion in the prestressing strands and reinforcing bars was quantitatively evaluated based on the charge transmitted through a specified circuit over a specified period, following Faraday's law. The methodology proposed in this study offers an accurate assessment of the corrosion characteristics observed in the prestressing strands and reinforcing bars. This study provided predictions of corrosion amount and depth for both types of reinforcements, depending on variations in the accelerated corrosion experiments. These findings are expected to aid in modeling corrosion in full-sized specimens, setting environmental parameters, and forecasting corrosion rates relative to the service life of the structures

Keywords Corrosion characteristics, Prestressing strand, Reinforcing bar, Structural safety, Faraday's law

1 Introduction

The safety of prestressed and reinforced concrete structures relies on the synergistic interaction between the concrete and the embedded prestressing strands and reinforcing bars, functioning as composite materials. In general, the predominant factor compromising the durability and safety of these structures is the corrosion of these reinforcing elements, rather than the deterioration of the concrete itself (Collins & Mitchell, 1991; Kim, 2022, 2023; Lignola et al., 2012; Xu et al., 2022).

*Correspondence:
Tae-Hoon Kim
thkim@krri.re.kr
[1] Advanced Railroad Civil Engineering Division, Korea Railroad Research Institute, 176, Cheoldobangmulgwan-Ro, Uiwang-Si 16105, Gyeonggi-Do, Korea
[2] Department of Civil and Environmental Engineering, University of Ulsan, 93, Daehak-Ro, Ulsan-Si 44610, Korea

Within the highly alkaline environment of concrete structures, characterized by a pH of 12–13, a protective passive film naturally forms around the prestressing strands and reinforcing bars, which serves to inhibit corrosion (Kwon & Na, 2011; Park et al., 2012; Zhang et al., 2010). If the concrete remains intact and free from cracks, it can effectively protect these reinforcing elements from corrosion. However, if cracks occur, they facilitate the easy entry of water, oxygen, and chloride ions, or cause neutralization effects on the embedded materials, damaging the protective film. This damage leads to accelerated corrosion, rapid structural deterioration, and the expansion of corrosion products that cause scaling and delamination of the concrete. Moreover, as corrosion-induced cracks widen, they allow oxygen and chloride ions to penetrate more easily, further accelerating the corrosion process. Consequently, the diminished bond between the concrete and its reinforcing

materials significantly compromises the durability and safety of the structures (Auyeung et al., 2000; Carvalho et al., 2018; Pantazopoulou & Papoulia, 2001; Shuxian et al., 2017). Once corrosion sets in, the repair or maintenance of these strands and bars becomes both challenging and costly. Therefore, the early detection of corrosion signs and the implementation of preventive maintenance measures are essential for maintaining the integrity of concrete structures.

Prestressing strands embedded in prestressed concrete structures are generally considered more resistant to corrosion and less prone to deterioration from cracks compared to those in reinforced concrete structures. However, prestressing strands in plastic ducts exposed to external environments have been found to be susceptible to corrosion (Dai et al., 2016). Contributing factors include ungrouted areas, damaged ducts, and the ingress of oxygen, water, and de-icing agents through anchoring devices from above. Corrosion of prestressing strands is deemed more critical than that of reinforcing bars, because these strands are constantly under high tensile stresses. Stress corrosion can occur in prestressing strands where materials are exposed to a corrosive environment and are under high tensile stress. Consequently, even with the same potential difference as reinforcing bars, prestressing strands exhibit lower specific resistance and higher corrosion currents, leading to a faster rate of corrosion (Li et al., 2011; Wang et al., 2014).

Prestressed concrete structures with corroded prestressing strands are more susceptible to a significant reduction in flexural strength owing to the premature failure of these strands, with stress corrosion and hydrogen embrittlement identified as major contributing factors (Jeon et al., 2019; MacDougall & Bartlett, 2002; Ramseyer & Kang, 2012). In addition, the corrosion of reinforcing bars reduces their cross-sectional area and induces concrete cracking. The corrosion products decrease the bond performance and affect the tensile hardening properties of the concrete. This degradation significantly affects the seismic performance and structural behavior of concrete structures (Belletti et al., 2020; Crespi et al., 2022; Li et al., 2017; Zucca et al., 2023).

Initially, as corrosion of reinforcing bars progresses, the bond strength between the concrete and the bars increases. However, as corrosion continues, the bond strength decreases owing to the loss of rib surface area on the reinforcing bars (Bastidas-Arteaga, 2018; Mohammed et al., 2018; Toongoenthong & Maekawa, 2005). Particularly from a seismic analysis perspective, deterioration such as corrosion alters dynamic characteristics, influencing the location and mode of initial failure and reducing seismic performance. Therefore, it is crucial to incorporate considerations of deterioration due to corrosion in precise seismic performance evaluations of structures affected by aging and other factors.

To assess the corrosion of prestressing strands and reinforcing bars in concrete, conducting experiments in an actual corrosive environment, supplemented by exposure experiments, proves effective. However, given that this process is time-consuming, an accelerated corrosion method is frequently used to quantitatively evaluate corrosion in prestressing strands and reinforcing bars over a shorter period. Research in this field is actively pursuing the assessment of corrosion using non-destructive methods, primarily focusing on measuring corrosion current density and corrosion potential through configurations of electrochemical sensors. The methodology proposed in this study offers an accurate assessment of the corrosion characteristics observed in the prestressing strands and reinforcing bars.

Consequently, this study aims to quantify the corrosion amount by inducing corrosion in prestressing strands and reinforcing bars embedded in mold-type concrete specimens. It also seeks to predict and examine the corrosion characteristics of prestressed and reinforced concrete structures.

2 Comparison of Corrosion Characteristics Between Prestressing Strands and Reinforcing Bars

Concrete is commonly considered a stable and long-lasting construction material. However, prestressing strands and reinforcing bars embedded within concrete are susceptible to corrosion, particularly when exposed to salt in marine environments or from prolonged use of de-icing agents. This corrosion leads to the gradual formation of cracks and spalling in the covering concrete, which reduces durability and ultimately compromises structural safety due to weakened structural strength (Wang et al., 2014).

Corrosion-related issues, such as a reduction in the cross-sectional area of prestressing strands and reinforcing bars, decreased bond strength, and concrete cracking, are critically important, because they significantly impact structural safety and can have substantial socio-economic implications. Corrosion is initiated by the penetration of chloride ions through cracks, which may result from drying shrinkage, thermal stress from hydration heat, and unexpected loading. This process leads to a reduction in bond strength, a decrease in the cross-sectional area of the reinforcing materials, weakening of the interface between concrete and reinforcement, and cover cracking due to the volumetric expansion of corrosion products. In addition, fatigue loads on such structures can induce the formation and expansion of micro-cracks in the concrete, potentially leading to structural failure under loads

lower than the design load (Darmawan & Stewart, 2007; Hanjari et al., 2011; Tapan & Aboutaha, 2009; Xu et al., 2021).

The most commonly used type of prestressing strand in construction is the 7-wire strand, as depicted in Fig. 1a, consisting of six wires twisted around a central wire in an S-outline lay. Corrosion can affect each of the seven wires and, in severe cases, may only impact one or a few wires. Therefore, localized corrosion in specific wires can significantly degrade the overall performance of the prestressing strands.

Deformed reinforcing bars, depicted in Fig. 1b, are commonly utilized due to their excellent bonding and anchoring properties, facilitated by their transverse and longitudinal ribs. As these bars function integrally within the concrete matrix, localized corrosion damage typically has a less pronounced impact on overall performance degradation compared to prestressing strands.

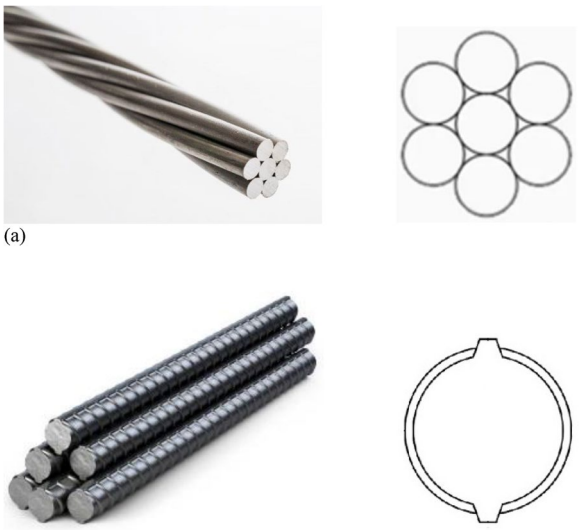

Fig. 1 Characteristics of reinforcement material: **a** Prestressing strand and **b** reinforcing bar

Faraday's law is primarily employed to assess the extent of corrosion in prestressing strands and reinforcing bars (Oh et al., 2016). The law is encapsulated in the following equation, which serves as the foundation for predicting the corrosion amount of steel:

$$M = \frac{c}{zF} \int q dt \tag{1}$$

where M denotes the corrosion amount (mol), z represents the ion number of iron (=2), F is the Faraday constant (=96,500 C), q is the current (mA), t is the measurement time (sec), and c is the experimental constant (=1). Note that 1 mol of iron (Fe) weighs 55.847 g.

3 Corrosion Experiment and Evaluation of Prestressing Strands

3.1 Corrosion Experiment of Prestressing Strands

As illustrated in Fig. 2, a prestressing strand with a diameter of 12.7 mm and a length of 250 mm was centrally placed within a mold specimen, which possesses a square cross section of 100 mm by 100 mm and a length of 200 mm. The strand extended 150 mm into the concrete, which was designed with a compressive strength of 40 MPa and the prestressing strand with a tensile strength of 1860 MPa. These parameters—diameter of the strands, and the compressive and tensile strengths of the concrete and strands, respectively—are typical values for prestressed concrete structures. The mix design is given in Table 1. The concrete mixture for mold specimens in Fig. 2 was composed of ordinary Portland cement, tap water, fine aggregates and coarse aggregates with maximum size of 25 mm.

To induce corrosion, the specimens were submerged in a 3% NaCl solution. The prestressing strands were connected to the positive pole and sacrificial reinforcing bars to the negative pole, establishing a corrosion-inducing circuit as depicted in Fig. 3. A DC power supply was used to consistently deliver a voltage of 20 V to the circuit, with a 10 W resistor connected to each specimen to ensure a steady current flow.

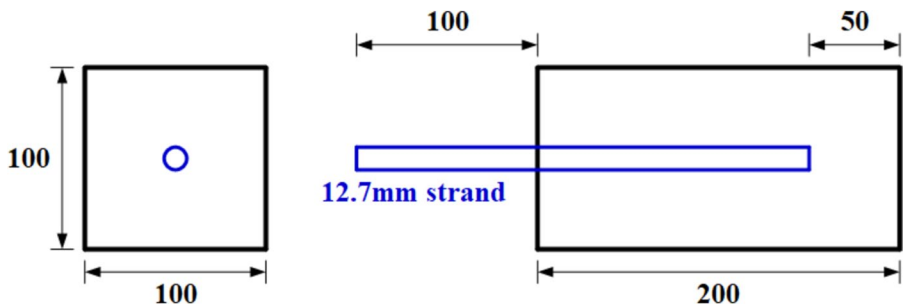

Fig. 2 Prestressing strand specimens (unit: mm)

Table 1 Composition of concrete mixture for prestressing strand specimens

Concrete class (MPa)	Slump (mm)	Cement (kg)	Fine aggregate (kg)	Coarse aggregate (kg)	Water (kg)	Water–cement ratio (%)
40	150	517	745	995	170	32.9

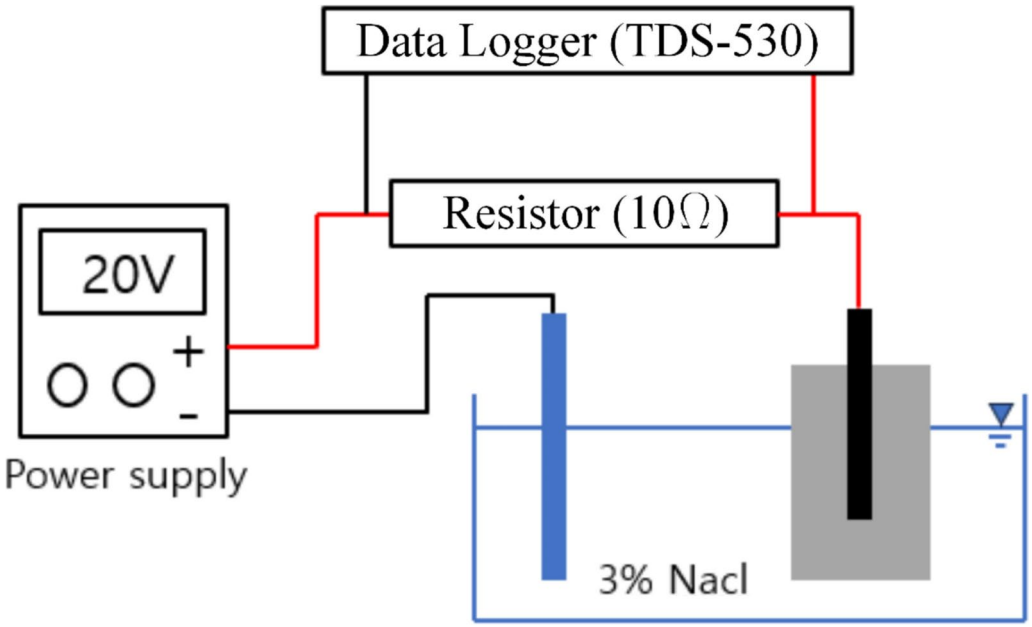

Fig. 3 Schematic diagram for corrosion acceleration

During the experiment, oxidation and reduction reactions occurred simultaneously on the specimen's surface, with both positive and negative currents flowing. Corrosion was facilitated by this current flow, and its extent was quantitatively determined using Faraday's law. To determine the accumulated current (A·sec) needed to achieve the desired corrosion amount, the voltage (V) across each specimen's resistor (W) was recorded hourly using a data logger. This voltage was then converted into current (A = V / W) and calculated using the quadrature method.

3.2 Evaluation of the Corrosion Amount in Prestressing Strands

To efficiently evaluate the corrosion amount in prestressing strands, a single tank setup was used to corrode a sacrificial reinforcing bar and six experimental specimens simultaneously, as shown in Fig. 4a. The accumulated current was monitored using a TDS-530 data logger, depicted in Fig. 4b. The corrosion amount was determined by measuring the average weight of three reference prestressing strands that had not been exposed to corrosion. These reference strands had an average weight of 194 g, with a nominal diameter of 12.7 mm and a length of 250 mm.

Figure 5 displays sample graphs of the current, converted from the voltage measured by the data logger for all 18 specimens. Figure 6 shows a similar graph, detailing the current derived from the voltage readings across sample specimens. A DC power supply provided a constant 20 V to each specimen, with the current delivered through a connected resistor. The voltage across these resistors was logged, and when cracks appeared on the concrete surface, the supplied current increased continuously. This increase was due to enhanced penetration of NaCl solution through the cracks, raising the voltage across the resistors.

Figure 7 displays images of the experimental samples that underwent corrosion over a 7-day period, each connected to a 10W resistor. Figure 8 illustrates the relationship between accumulated current and corrosion time. On day 6, the average accumulated current reached 80,346 A·sec, correlating with a corrosion level of 10.88%. By day 7, the average accumulated current increased to 87,252 A·sec, with the corrosion level rising to 14.05%.

Figure 9 displays a comparison of the experimental corrosion levels of prestressing strands with theoretical

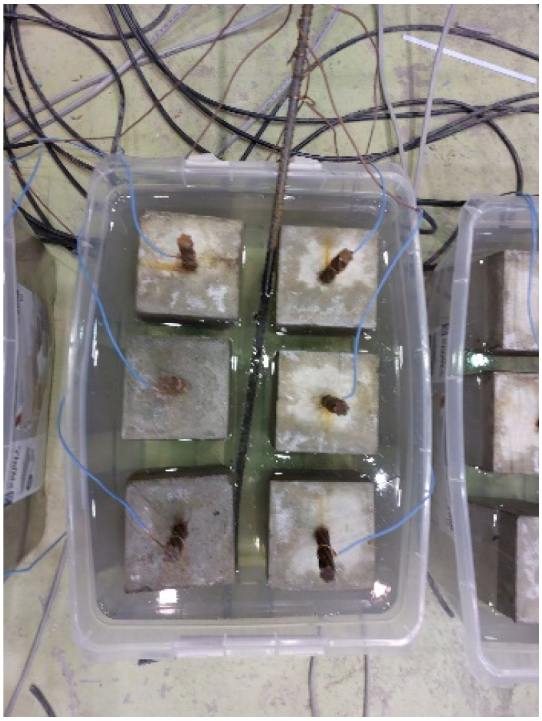

(a)

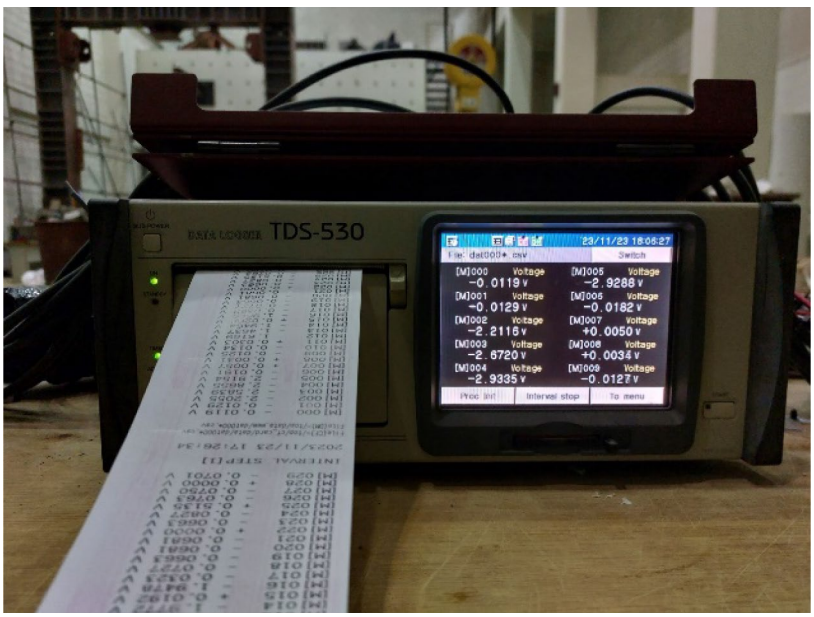

(b)

Fig. 4 Photo for corrosion acceleration setting: **a** specimens and **b** data logger

values calculated using Faraday's law, as described previously, relative to the accumulated current. At an accumulated current of 79,955 A·sec, the experimental corrosion level is recorded at 12.89%, versus a theoretical level of 19.89%. When the accumulated current increases to 111,818 A·sec, the experimental level rises to 21.47%,

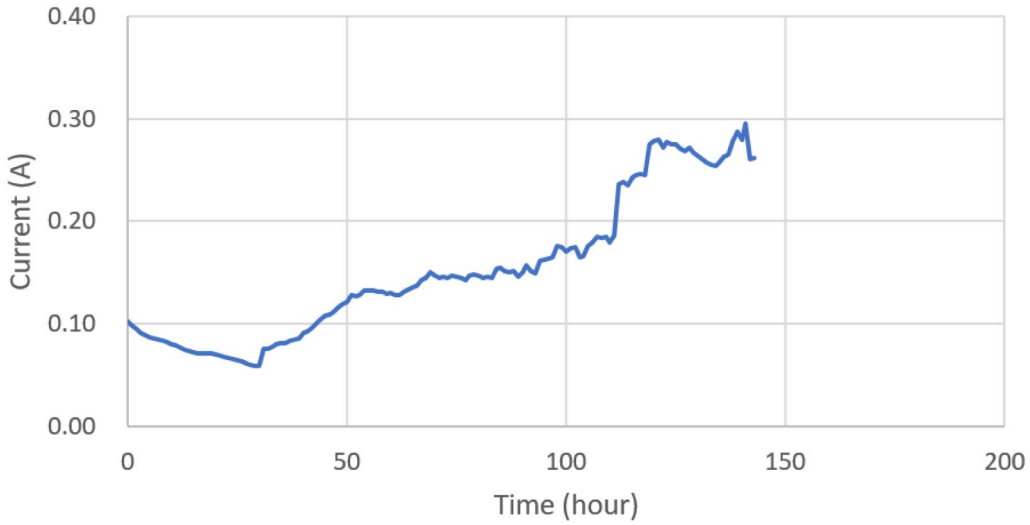

(a)

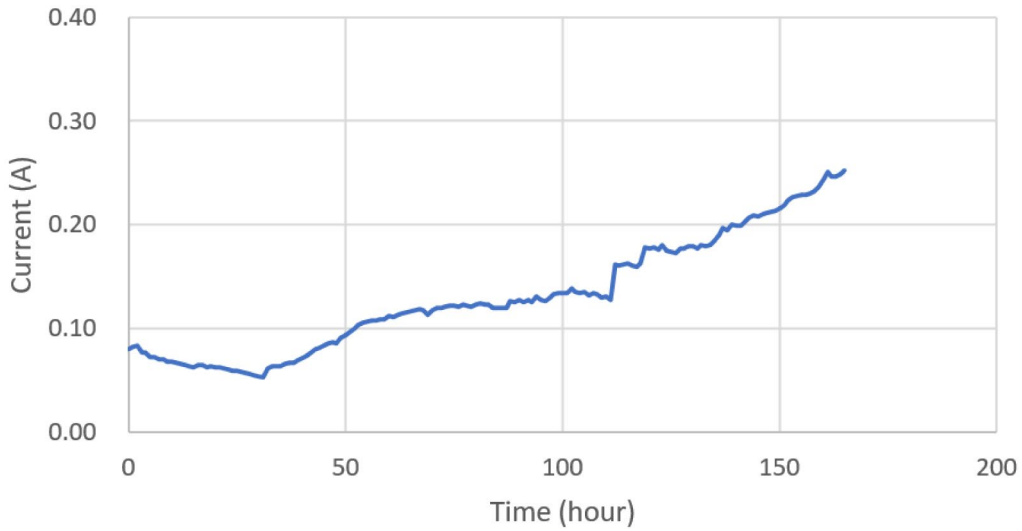

(b)

Fig. 5 Sample of accelerating of corrosion for prestressing strand: (**a**) Specimen 2 and (**b**) Specimen 14

compared to a theoretical level of 27.84%. At 134,521 A·sec, the experimental corrosion level reaches 26.63%, whereas the theoretical level is 33.56%. These results indicate that as the accumulated current increases, so does the corrosion level; however, the experimental values consistently fall below the theoretical predictions. In the evaluations, each of the 7-wire strands in the configuration, consisting of six strands twisted around a central wire in an S-lay, experienced corrosion, with notable concentration on several strands, as illustrated in Fig. 10.

Figure 11 presents a comparison of the experimental corrosion depth of prestressing strands with theoretical values derived using Faraday's law, related to the accumulated current. The corrosion depth was geometrically determined by considering the corrosion level (%) in relation to the nominal diameter of 12.7 mm.

At an accumulated current of 79,955 A·sec, the experimental corrosion depth measures 0.42 mm, in contrast to a theoretical depth of 0.67 mm. When the current reaches 111,818 A·sec, the experimental depth is 0.72 mm, compared to the theoretical depth of 0.96 mm. At 134,521 A·sec, the experimental depth increases to 0.91 mm, while the theoretical depth is 1.17 mm. Similar to the corrosion level data, the experimental corrosion

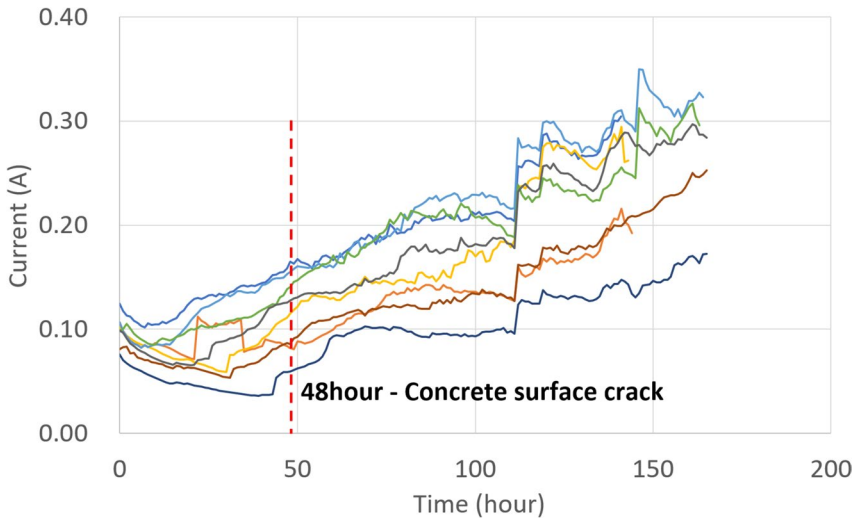

Fig. 6 Changes in current for prestressing strand

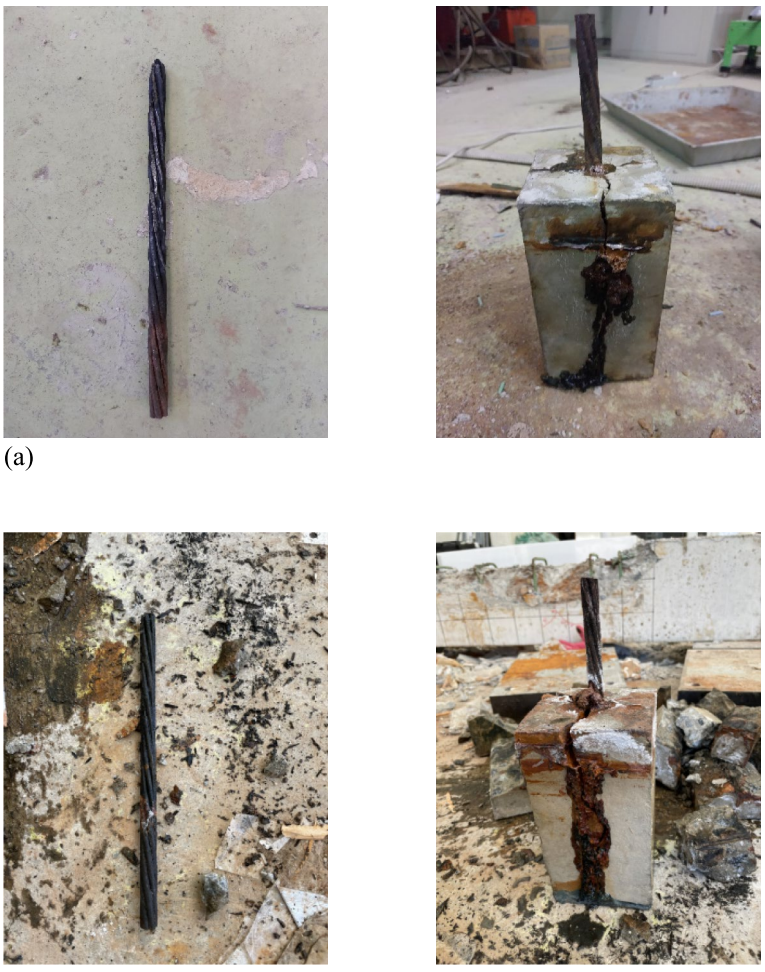

Fig. 7 Sample of accelerating of corrosion for prestressing strand: (**a**) 144 h (6 days) and (**b**) 168 h (7 days)

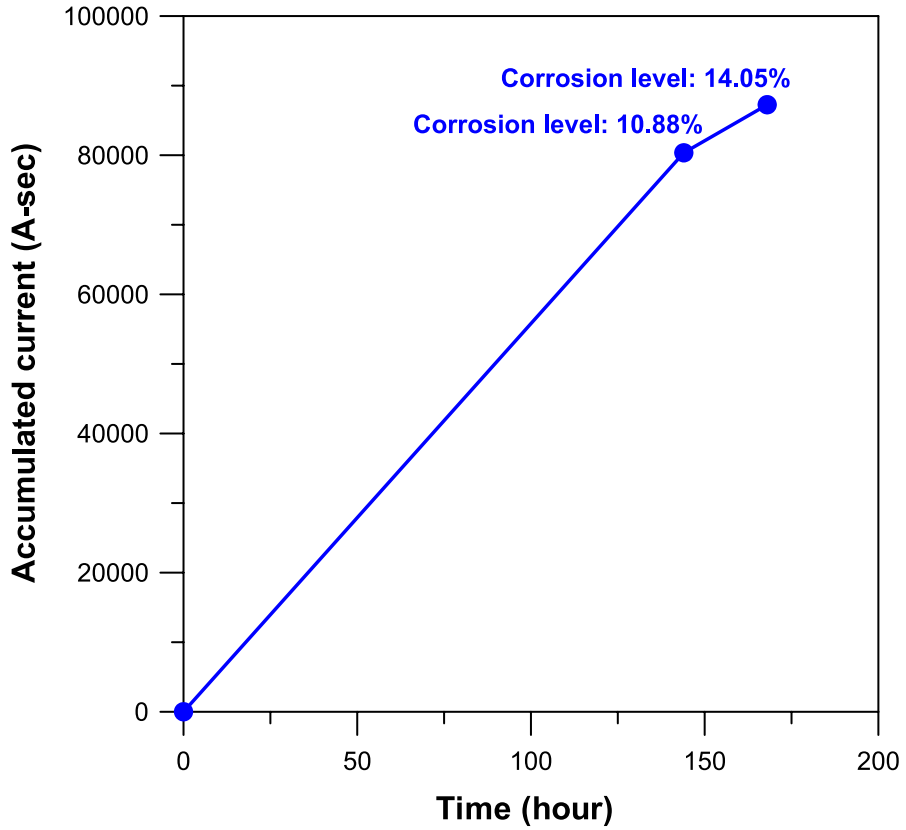

Fig. 8 Accumulated current for prestressing strand in test period

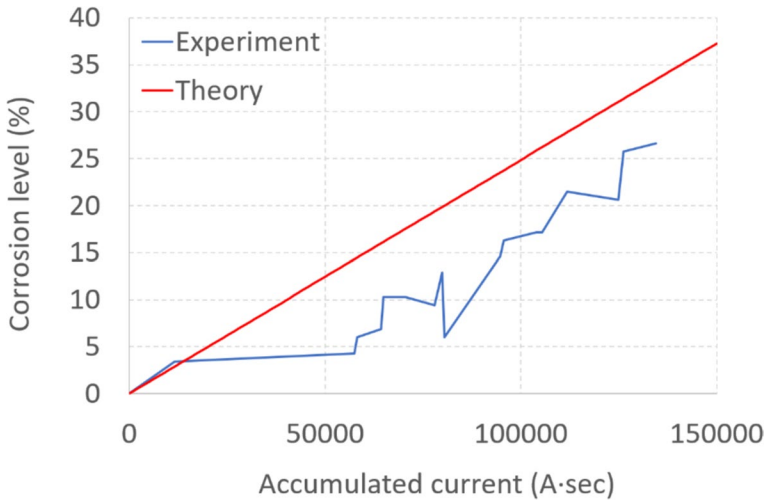

Fig. 9 Corrosion level variation for prestressing strand with accumulated current

depth consistently registers lower than the theoretical values for equivalent currents. As with the corrosion level assessment, each of the 7-wire strands was affected in this analysis, with corrosion notably concentrated on several of the strands arranged in an S-lay configuration.

4 Corrosion Experiment and Evaluation of Reinforcing Bars

4.1 Corrosion Experiment of Reinforcing Bars

Similar to the prestressing strands, the corrosion experiment for reinforcing bars involved inserting one H19 reinforcing bar, 250 mm in length, into the center of a mold specimen. The mold had a square cross section measuring 100 mm by 100 mm and a height of 200 mm, as depicted in Fig. 12. The reinforcing bar was embedded 150 mm into the concrete, which was designed with a compressive strength of 27 MPa and a yield strength of 400 MPa for the bar. These parameters—the diameter of

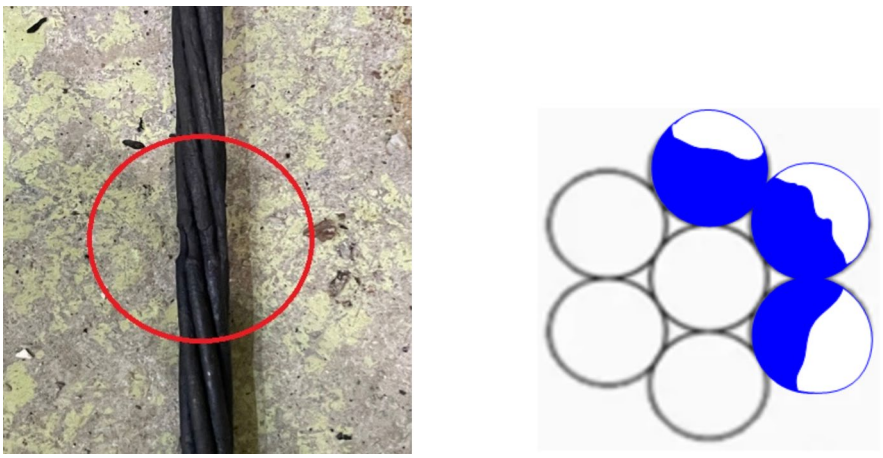

Fig. 10 Cross section of a corroded prestressing strand

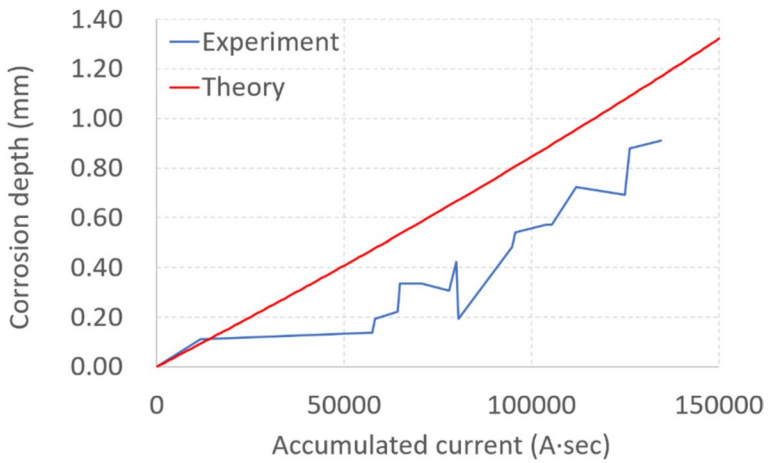

Fig. 11 Corrosion depth variation for prestressing strand with accumulated current

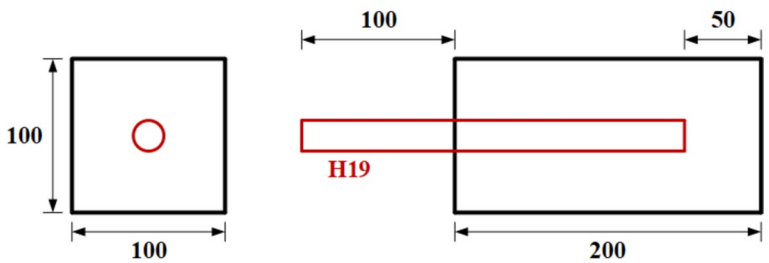

Fig. 12 Reinforcing bar specimens (unit: mm)

Table 2 Composition of concrete mixture for reinforcing bar specimens

Concrete class (MPa)	Slump (mm)	Cement (kg)	Fine aggregate (kg)	Coarse aggregate (kg)	Water (kg)	Water–cement ratio (%)
27	150	333	821	940	163	48.9

the reinforcing bar, the compressive strength of the concrete, and the yield strength of the bar—are representative of typical values for reinforced concrete structures. The mix design is given in Table 2. The concrete mixture for mold specimens in Fig. 12 was composed of ordinary Portland cement, tap water, fine aggregates and coarse aggregates with maximum size of 25 mm.

To induce corrosion, the specimens were immersed in a 3% NaCl solution. The reinforcing bar was connected to the positive pole and sacrificial reinforcing bars to the negative pole, creating a corrosion-inducing circuit as illustrated in Fig. 3 from the previous section. A DC power supply consistently delivered a voltage of 20 V, with a 10 W resistor connected to each specimen to ensure a stable current flow.

Oxidation and reduction reactions occurred simultaneously on the surface of the specimen, with currents flowing in both positive and negative directions. Corrosion resulted from this bidirectional current flow. Faraday's law was employed to assess the corrosion amount. To determine the accumulated current (A·sec) needed to achieve the desired corrosion level, the voltage (V) across the resistor (W) of each specimen was measured hourly using a data logger. This voltage was then converted into current (A = V / W) and calculated using the quadrature method.

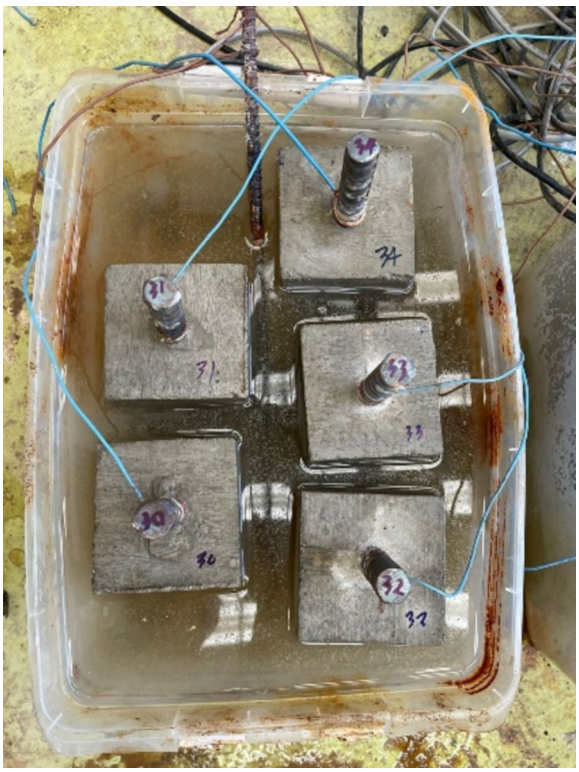

Fig. 13 Photo for corrosion acceleration for reinforcing bar

4.2 Evaluation of the Corrosion Amount in Reinforcing Bars

To evaluate the corrosion amount in reinforcing bars, a sacrificial bar and five experimental specimens were simultaneously corroded in a single tank, as depicted in Fig. 13. The accumulated current was monitored using a TDS-530 data logger, shown in Fig. 4b. The corrosion amount was determined by measuring the average weight of three uncorroded reinforcing bars, which was found to be 337.5 g, with a nominal diameter of 19.1 mm and a length of 250 mm.

Figure 14 displays sample graphs of the current, derived from the voltage readings recorded by the data logger for all 40 specimens at various target corrosion levels.

Figure 15 illustrates the graph of current, converted from the voltage measured by the data logger for all specimens. A constant voltage of 20 V was maintained by a DC power supply, with the current to each specimen transmitted through a connected resistor. The voltage across these resistors is continuously logged. As cracks develop on the concrete surface, there is a steady increase in the supplied current, evidenced by the rising voltage across the resistors. This increase is attributed to the enhanced penetration of NaCl solutions through the cracks, similar to observations made with prestressing strands in the previous section.

Figure 16 presents images of the experimental samples subjected to corrosion over 18 days, with a 10 W resistor connected to each of the 40 specimens. In addition, Fig. 17 charts the accumulated current in relation to corrosion-induced time. By day 3, the accumulated current reaches 54,529 A·sec, corresponding to a corrosion level of 9.11%; by day 7, it increases to 117,813 A·sec, with a corrosion level of 12.37%. By day 14, the accumulated current escalates to 350,479 A·sec, with the corrosion level at 27.78%; and by day 18, it peaks at 540,707 A·sec, marking a corrosion level of 45.48%.

Figure 18 presents a comparison of the experimental corrosion levels of reinforcing bars with theoretical

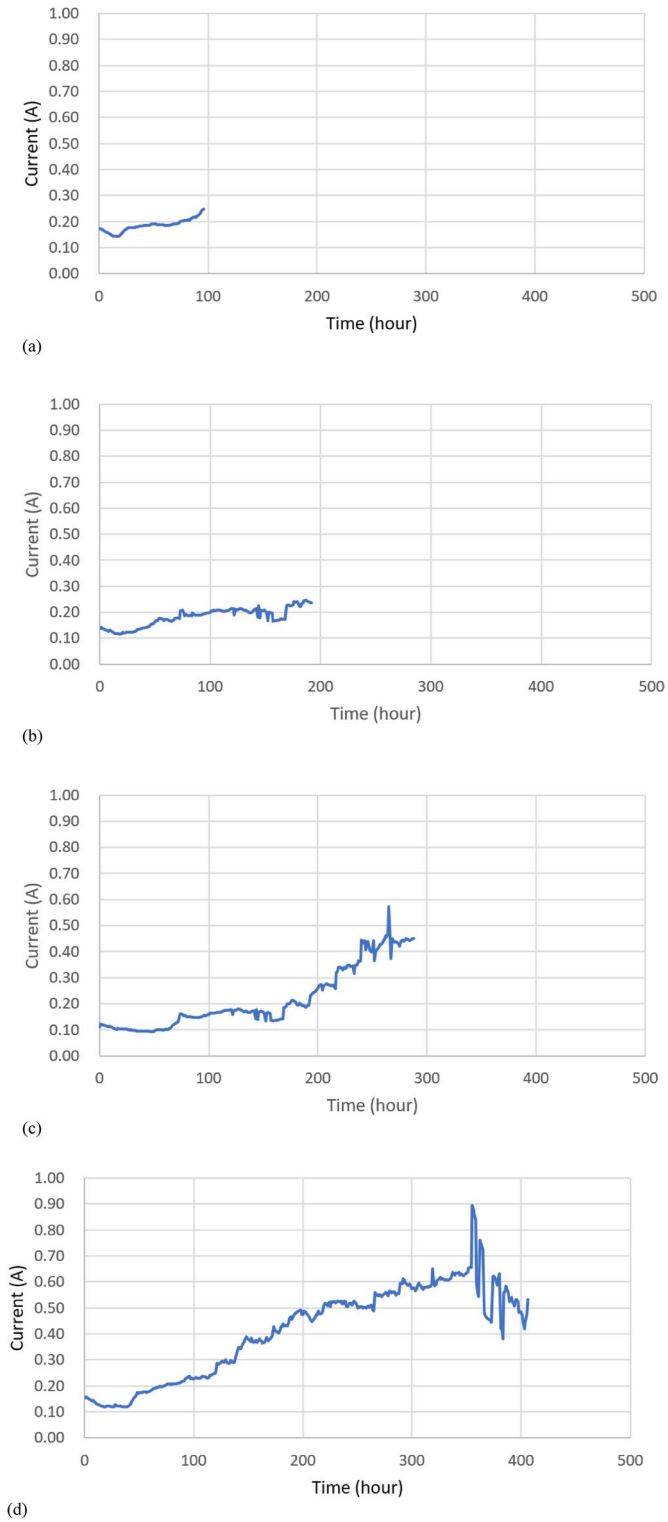

Fig. 14 Sample of accelerating of corrosion for reinforcing bar: (**a**) Specimen 29, (**b**) Specimen 1, (**c**) Specimen 10 and (**d**) Specimen 28

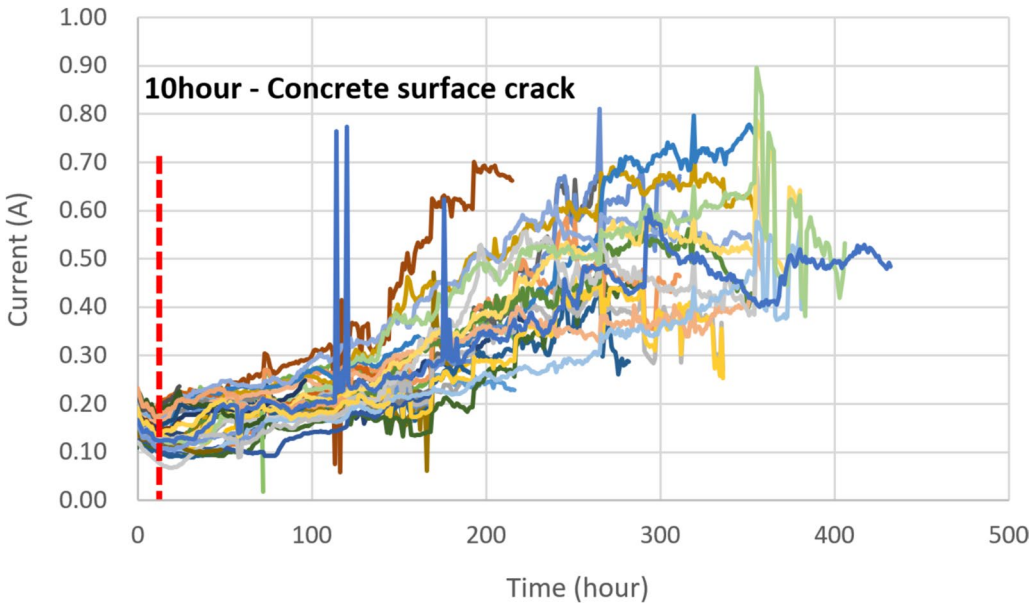

Fig. 15 Changes in current for reinforcing bar

values calculated using Faraday's law, as previously described, relative to the accumulated current.

At an accumulated current of 204,011 A·sec, the experimental corrosion level is measured at 20.22%, slightly exceeding the theoretical value of 17.49%. When the accumulated current reaches 392,931 A·sec, the experimental level is 32.37%, closely matching the theoretical prediction of 33.69%. Finally, at 599,180 A·sec, the experimental corrosion level is 47.26%, slightly below the theoretical level of 51.36%. This data indicates that as the accumulated current increases, so does the corrosion level, with the experimental values closely tracking the theoretical predictions.

Figure 19 offers a comparison of the experimental corrosion depths of reinforcing bar ribs with theoretical values, also derived using Faraday's law. The corrosion depth is geometrically determined based on the corrosion level (%) in relation to the rib's nominal diameter of 19.1 mm.

At an accumulated current of 204,011 A·sec, the experimental corrosion depth is 1.02 mm, compared to the theoretical depth of 0.88 mm. At 392,931 A·sec, the experimental depth is 1.70 mm, nearly aligning with the theoretical depth of 1.77 mm. When the accumulated current reaches 599,180 A·sec, the experimental depth is 2.61 mm, just shy of the theoretical depth of 2.89 mm. As the accumulated current increases, so does the corrosion depth, with experimental measurements demonstrating a trend similar to the theoretical values, closely reflecting changes relative to the rib's nominal diameter of 19.1 mm.

Figure 20 presents a comparison of the experimental corrosion depths of the part without ribs against theoretical values, calculated using Faraday's law as detailed in the previous section, in relation to the accumulated current. The corrosion depth was geometrically determined by considering the corrosion level (%) in relation to the diameter of 18.05 mm for the part without ribs.

At an accumulated current of 204,011 A·sec, the experimental corrosion depth measures 0.96 mm, slightly surpassing the theoretical depth of 0.83 mm. As the current increases to 392,931 A·sec, the experimental depth is 1.60 mm, closely approaching the theoretical value of 1.67 mm. When the current further escalates to 599,180 A·sec, the experimental depth reaches 2.47 mm, compared to a theoretical depth of 2.73 mm. These results indicate that as the accumulated current rises, so does the corrosion depth. The experimental corrosion depths observed are similar to the theoretical predictions, closely corresponding to the diameter (18.05 mm) of the part without ribs.

5 Conclusions

In this study, mold-type specimens of prestressing strands and reinforcing bars were prepared to investigate and quantify the corrosion characteristics of these materials, which critically influence the durability and safety of

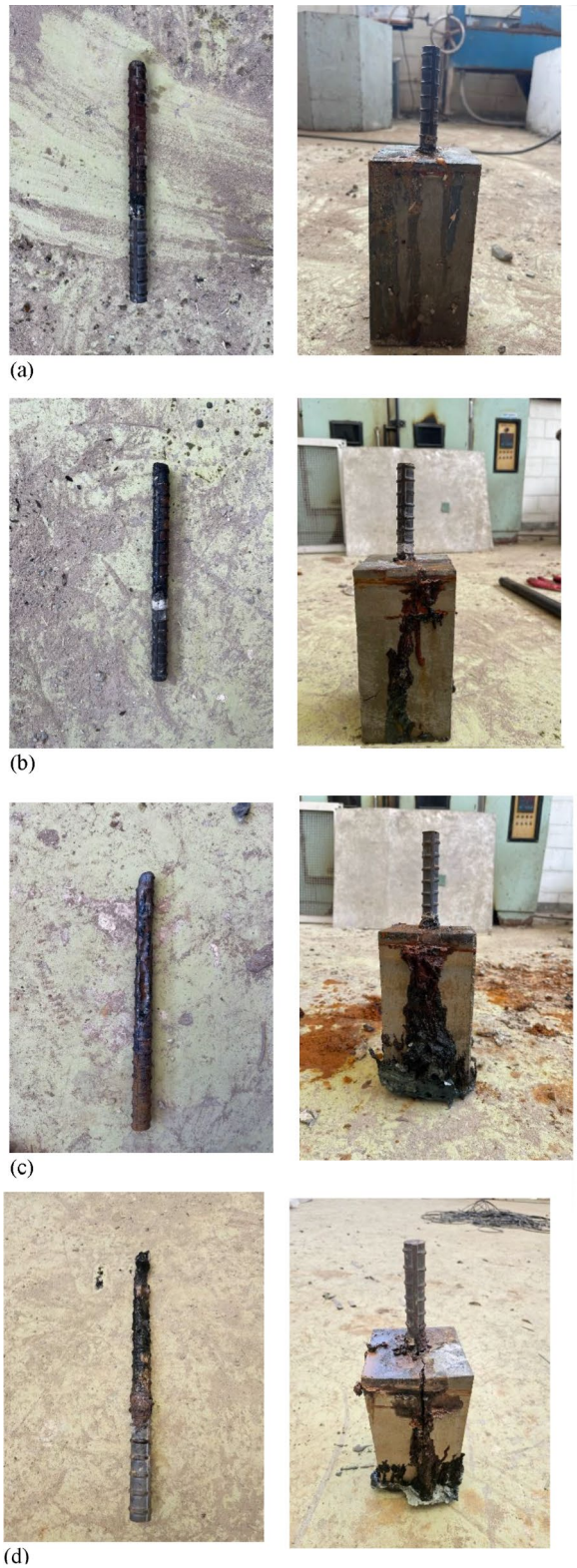

Fig. 16 Sample of accelerating of corrosion for reinforcing bar: (**a**) 72 h (3 days), (**b**) 168 h (7 days), (**c**) 336 h (14 days) and (**d**) 432 h (18 days)

prestressed and reinforced concrete structures. The corrosion process was accelerated using a specially designed experimental setup, and a total of 18 prestressing strand specimens and 40 reinforcing bar specimens were quantitatively evaluated, yielding the following insights:

(1) By integrating a mathematical model based on Faraday's law with results from accelerated corrosion experiments, this study developed a method for quantifying corrosion in concrete structures that incorporate prestressing strands and reinforcing bars. Moreover, the study especially provided predictions of corrosion amount and depth for both types of reinforcements, depending on variations in the accelerated corrosion experiments. These findings are expected to aid in modeling corrosion in full-sized specimens, setting environmental parameters, and forecasting corrosion rates relative to the service life of the structures.

(2) For prestressing strands, the experimentally determined corrosion levels were consistently lower than the theoretical values at equivalent accumulated currents. The analysis revealed that each of the 7-wire strands was affected, particularly noting that corrosion was concentrated on several strands of the six twisted around a central wire in an S-lay configuration. Conversely, for reinforcing bars, both with and without ribs, the experimental results closely matched the theoretical predictions. This suggests that the theoretical model, based on Faraday's law, is more accurately applicable to single reinforcing bar structures than to complex prestressing strands composed of multiple wires.

(3) The developed method for quantifying corrosion in prestressing strands and reinforcing bars in concrete structures is vital for maintenance and routine inspections. It provides essential data for determining the optimal timing and methods for maintenance and reinforcement and for predicting long-term performance degradation. In prestressing strands, stress corrosion due to high stress levels and inadequate grouting within ducts can create voids. These voids facilitate the entry of chloride ions, underscoring the necessity of implementing effective corrosion prevention measures.

(4) This research also explored the effects of deterioration by focusing on the corrosion characteristics of bonded prestressing strands and reinforcing bars and quantifying their corrosion amounts. Future studies will aim to extend this investigation to eval-

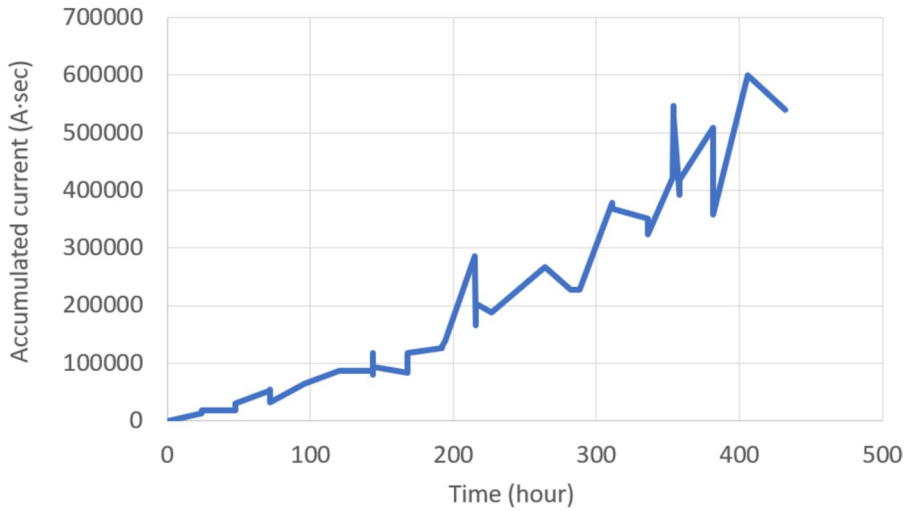

Fig. 17 Accumulated current for reinforcing bar in test period

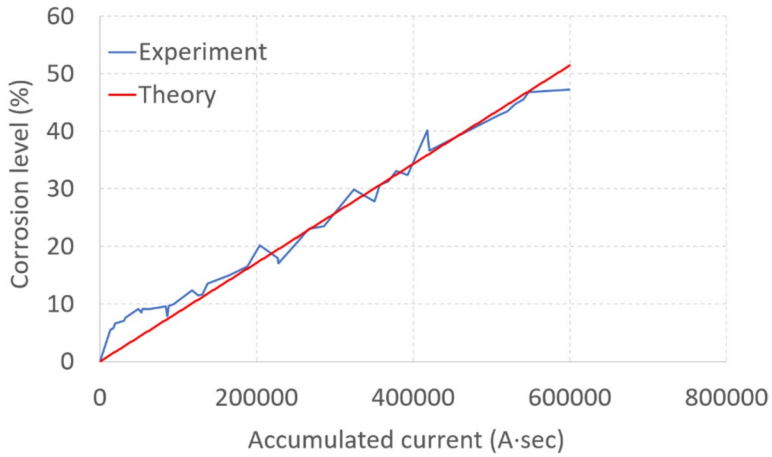

Fig. 18 Corrosion level variation for reinforcing bar with accumulated current

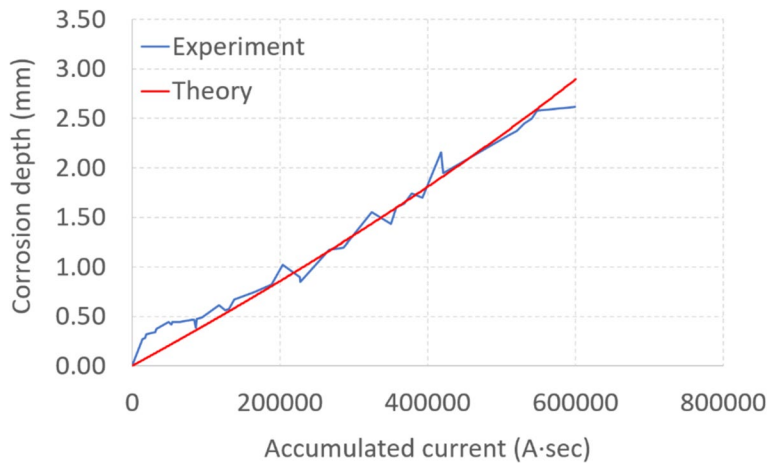

Fig. 19 Corrosion depth variation for reinforcing bar with accumulated current (with ribs)

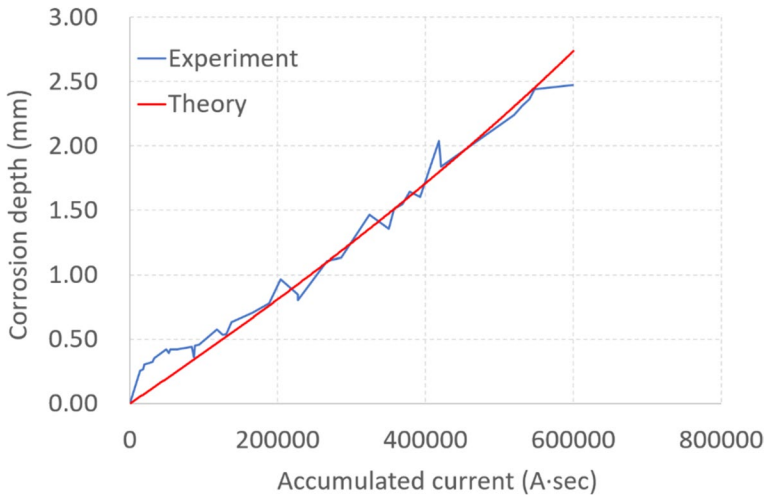

Fig. 20 Corrosion depth variation for reinforcing bar with accumulated current (without ribs)

uate the corrosion properties and quantities of non-bonded prestressing strands, considering additional factors such as sheath defects or inadequate grouting. In addition, the influence of the bond strength between corroded prestressing strands or reinforcing bars and concrete for element levels and structural levels will be explored.

Acknowledgements
This research was supported by a grant from R&D Program (Development of Core Technologies for Creating New Railroad Industries, PK2404B2) of the Korea Railroad Research Institute.

Author contributions
THK planed this paper, analyzed the experimental results, proposed the accurate assessment method. KYE analyzed the experimental results. CHS analyzed the experimental results. IHK proposed the accurate assessment method. All authors read and approved the final manuscript.

Funding
This research was supported by a grant from R&D Program (Development of Core Technologies for Creating New Railroad Industries, PK2404B2) of the Korea Railroad Research Institute.

Availability of data and materials
The research data used to support the finding of this study are described and included in the article. Furthermore, some of the data used in this study are also supported by providing references as described in the article.

Declarations

Competing interests
The author declares no competing interests.

Received: 21 August 2024 Accepted: 25 December 2024
Published online: 02 April 2025

References

Auyeung, Y. B., Balaguru, P., & Chung, L. (2000). Bond behavior of corroded reinforcement bars. *ACI Materials Journal, 97*(2), 214–220. https://doi.org/10.14359/826

Bastidas-Arteaga, E. (2018). Reliability of reinforced concrete structures subjected to corrosion-fatigue and climate change. *International Journal of Concrete Structures and Materials, 12*(1), 77–89. https://doi.org/10.1186/s40069-018-0235-x

Belletti, B., Rodriguez, J., Andrade, C., Franceschini, L., Montero, J. S., & Vecchi, F. (2020). Experimental tests on shear capacity of naturally corroded prestressed beams. *Structural Concrete, 21*(5), 1777–1793. https://doi.org/10.1002/suco.202000205

Carvalho, E. P., Miranda, M. P., Fernandes, D. S. G., & Alves, G. V. (2018). Comparison of test methodologies to evaluate steel-concrete bond strength of thin reinforcing bar. *Construction and Building Materials, 183*, 243–252. https://doi.org/10.1016/j.conbuildmat.2018.06.109

Collins, M. P., & Mitchell, P. (1991). *Prestressed Concrete Structure*. Prentice Hall.

Crespi, P., Zucca, M., Valente, M., & Longarini, N. (2022). Influence of corrosion effects on the seismic capacity of existing RC bridges. *Engineering Failure Analysis, 140*, 106546. https://doi.org/10.1016/j.engfailanal.2022.106546

Dai, L., Wang, L., Zhang, J., & Zhang, X. (2016). A global model for corrosion-induced cracking in prestressed concrete structures. *Engineering Failure Analysis, 62*, 263–275. https://doi.org/10.1016/j.engfailanal.2016.01.013

Darmawan, M. S., & Stewart, M. S. (2007). Effect of pitting corrosion on capacity of prestressing wires. *Magazine of Concrete Research, 59*(2), 131–139. https://doi.org/10.1680/macr.2007.59.2.131

Hanjari, K. Z., Kettil, P., & Lundgren, K. (2011). Analysis of mechanical behavior of corroded reinforced concrete structures. *ACI Structural Journal, 108*(5), 532–541. https://doi.org/10.14359/51683210

Jeon, C.-H., Lee, J.-B., Lon, S., & Shim, C.-S. (2019). Equivalent material model of corroded prestressing steel strand. *Journal of Materials Research and Technology, 8*(2), 2450–2460. https://doi.org/10.1016/j.jmrt.2019.02.010

Kim, T.-H. (2022). Seismic performance assessment of deteriorated two-span reinforced concrete bridges. *International Journal of Concrete Structures and Materials*. https://doi.org/10.1186/s40069-022-00498-9

Kim, T.-H. (2023). Analytical performance assessment of deteriorated pre-stressed concrete beams. *International Journal of Concrete Structures and Materials*. https://doi.org/10.1186/s40069-023-00624-1

Kwon, S. J., & Na, U. J. (2011). Prediction of durability for RC columns with crack and joint under carbonation based on probabilistic approach. *International Journal of Concrete Structures and Materials, 5*(1), 11–18. https://doi.org/10.4334/IJCSM.2011.5.1.011

Li, F., Luo, X., & Liu, Z. (2017). Corrosion of anchorage head system of post-tensioned prestressed concrete structures under chloride environment. *Structural Concrete, 18*(6), 902–913. https://doi.org/10.1002/suco.201600140

Li, F., Yuan, Y., & Li, C.-Q. (2011). Corrosion propagation of prestressing steel strands in concrete subject to chloride attack. *Construction and Building Materials, 25*(10), 3878–3885. https://doi.org/10.1016/j.conbuildmat.2011.04.011

Lignola, G. P., Ludovico, M. D., Prota, A., & Manfredi, G. (2012). FRP prestressed concrete structures. *Wiley Encyclopedia of Composites*. https://doi.org/10.1002/9781118097298.weoc218

MacDougall, C., & Bartlett, F. M. (2002). Tests of corroded unbonded seven-wire strands with broken wires. *ACI Structural Journal, 99*(6), 803–810. https://doi.org/10.14359/12345

Mohammed, A. A., Hamdi, A. A., Alfarabi, M. S., Shamsad, A., & Mohammad, H. B. (2018). Finite element modeling of corroded RC beams using cohesive surface bonding approach. *Computers & Concrete, 22*(2), 167–182. https://doi.org/10.1298/cac.2018.22.2.167

Oh, K. S., Moon, J. M., Park, K. T., & Kwon, S. J. (2016). Evaluation of load capacity reduction in RC beam with corroded FRP hybrid bar and steel. *Journal of the Korea Institute for Structural Maintenance and Inspection, 20*(2), 10–17. https://doi.org/10.1111/jksmi.2016.20.2.010

Pantazopoulou, S. J., & Papoulia, K. D. (2001). Modeling cover-cracking due to reinforcement corrosion in RC structures. *Journal of Engineering Mechanics, ASCE, 127*, 342–351. https://doi.org/10.1061/(ASCE)0733-9399(2001)127:4(342)

Park, S. S., Kwon, S. J., & Jung, S. H. (2012). Analysis technique for chloride penetration in cracked concrete using equivalent diffusion and permeation. *Construction and Building Materials, 29*, 183–192. https://doi.org/10.1016/j.conbuildmat.2011.09.019

Ramseyer, C., & Kang, T.H.-K. (2012). Post-damage repair of prestressed concrete girders. *International Journal of Concrete Structures and Materials, 6*(3), 199–207. https://doi.org/10.1007/s40069-012-0019-7

Shuxian, H., Herbert, W., Rosemarie, H., Biqin, D., Peng, D., & Feng, X. (2017). Long-term monitoring of reinforcement corrosion in concrete using ground penetrating radar. *Corrosion Science, 114*(1), 123–132. https://doi.org/10.1016/j.corsci.2016.11.003

Tapan, M., & Aboutaha, R. S. (2009). Load carrying capacity of deteriorated reinforced concrete columns. *Computers & Concrete., 6*(6), 473–490. https://doi.org/10.12989/cac.2009.6.6.473

Toongoenthong, K., & Maekawa, K. (2005). Multi-mechanical approach to structural performance assessment of corroded RC members in shear. *Journal of Advanced Concrete Technology, 3*(1), 107–122. https://doi.org/10.3151/jact.3.107

Wang, L., Zhang, X., Zhang, J., Ma, Y., Xiang, Y., & Liu, Y. (2014). Effect of insufficient grouting and strand corrosion on flexural behavior of PC beams. *Construction and Building Materials, 53*, 213–224. https://doi.org/10.1016/j.conbuildmat.2013.11.069

Xu, J.-G., Cai, Z.-K., & Feng, D.-C. (2021). Life-cycle seismic performance assessment of aging RC bridges considering multi-failure modes of bridge columns. *Engineering Structures, 244*, 112818. https://doi.org/10.1016/j.engstruct.2021.112818

Xu, J.-G., Feng, D.-C., Mangalathu, S., & Jeon, J.-S. (2022). Data-driven rapid damage evaluation for life-cycle seismic assessment of regional reinforced concrete bridges. *Earthquake Engineering and Structural Dynamics, 51*(11), 2730–2751. https://doi.org/10.1002/eqe.3699

Zhang, R., Castel, A., & Francois, R. (2010). Concrete cover cracking with reinforcement corrosion of RC beams during chloride-induced corrosion process. *Cement and Concrete Research, 40*(3), 415–425. https://doi.org/10.1016/j.cemconres.2009.09.026

Zucca, M., Reccia, E., Longarini, N., Eremeyev, V., & Crespi, P. (2023). On the structural behaviour of existing RC bridges subjected to corrosion effects: Numerical insight. *Engineering Failure Analysis, 152*, 107500. https://doi.org/10.1016/j.engfailanal.2023.107500

Publisher's Note

Tae-Hoon Kim is a Principal Researcher in the Advanced Railroad Civil Engineering Division at the Korea Railroad Research Institute, Uiwang-si, Korea. He received his PhD in structural engineering from Sungkyunkwan University, Seoul, Korea. His research interests include nonlinear analysis and design of concrete structures, constitutive modeling, and seismic performance assessment.

Ki-Young Eum is a Chief Researcher in the Advanced Railroad Civil Engineering Division at the Korea Railroad Research Institute,Uiwang-si, Korea. He received his PhD in railway construction safety engineering from the Seoul National University of Science and Technology, Seoul, Korea. His research interests include railway construction safety.

Chang-Ho Sun is a Research Professor in the Department of Civil and Environmental Engineering at University of Ulsan, Ulsan-si, Korea. He received his PhD in structural engineering from the University of Ulsan, Ulsan-si, Korea. His research interests include behavior, analysis, and design of reinforced and prestressed concrete structures.

Ick-Hyun Kim is a Professor in the Department of Civil and Environmental Engineering at University of Ulsan, Ulsan-si, Korea. He received his PhD in structural engineering from the University of Tokyo, Tokyo, Japan. His research interests include behavior, analysis, and design of reinforced and prestressed concrete structures.